Development 129, 1657-1668 (2002)
Printed in Great Britain © The Company of Biologists Limited 2002
DEV2817

Disruption of mesodermal enhancers for *Igf2* in the minute mutant

Karen Davies[1], Lucy Bowden[1,*], Paul Smith[1], Wendy Dean[1], David Hill[2], Hiroyasu Furuumi[3], Hiroyuki Sasaki[3], Bruce Cattanach[4] and Wolf Reik[1,†]

[1]Laboratory of Developmental Genetics and Imprinting, Developmental Genetics Programme, Babraham Institute, Cambridge CB2 4AT, UK
[2]Lawson Health Research Institute, St. Joseph's Health Care, 268 Grosvenor Street, London, Ontario N6A4V2, Canada
[3]Division of Human Genetics, Department of Integrated Genetics, National Institute of Genetics, Graduate University for Advanced Studies, Mishima, Shizuoka 411-8540, Japan
[4]Medical Research Council, Mammalian Genetics Unit, Harwell, Didcot OX11 0RD, UK
*Present address: Gardiner-Caldwell Communications, The Towers, Park Green, Macclesfield SK11 7NG, UK
†Author for correspondence (e-mail: wolf.reik@bbsrc.ac.uk)

Accepted 26 December 2001

SUMMARY

The radiation-induced mutation minute (*Mnt*) in the mouse leads to intrauterine growth retardation with paternal transmission and has been linked to the distal chromosome 7 cluster of imprinted genes. We show that the mutation is an inversion, whose breakpoint distal to *H19* disrupts and thus identifies an enhancer for *Igf2* expression in skeletal muscle and tongue, and separates the gene from other mesodermal and extra-embryonic enhancers. Paternal transmission of *Mnt* leads to drastic downregulation of *Igf2* transcripts in all mesodermal tissues and the placenta. Maternal transmission leads to methylation of the *H19* differentially methylated region (DMR) and silencing of *H19*, showing that elements 3′ of *H19* can modify the maternal imprint. Methylation of the maternal DMR leads to biallelic expression of *Igf2* in endodermal tissues and foetal overgrowth, demonstrating that methylation in vivo can open the chromatin boundary upstream of *H19*. Our work shows that most known enhancers for *Igf2* are located 3′ of *H19* and establishes an important genetic paradigm for the inheritance of complex regulatory mutations in imprinted gene clusters.

Key words: Mouse, *Igf2*, *H19*, Imprinted genes

INTRODUCTION

Imprinted genes are expressed from one of the parental chromosomes only and have important roles in mammalian development, including in the control of foetal growth, placental development and behaviour after birth (Brannan and Bartolomei, 1999; Ferguson-Smith and Surani, 2001; Reik and Walter, 2001; Tilghman, 1999). Imprinted genes are regulated by epigenetic modifications, including DNA methylation, that originate in the parental germlines and are further elaborated after fertilisation. Several elements have recently been identified that contribute to the regulation of imprinted genes, including enhancers, promoters, silencers and chromatin boundary elements. Of these, promoters, silencers and boundary elements have been shown to be regulated epigenetically, leading to gene silencing or activation selectively on one allele. Many imprinted genes occur in clusters in which they can share some of these regulatory elements.

A large cluster of imprinted genes in the mouse is located on distal chromosome 7 and contains at least 15 imprinted transcripts (Reik and Walter, 2001). Genes in this cluster are particularly important for the control of foetal growth and placental development. The human orthologues of these genes are implicated in growth disorders and cancer (Feinberg, 2000; Maher and Reik, 2000; Tycko, 2000). Within this domain, the paternally expressed *Igf2* gene and the closely linked maternally expressed *H19* gene provide a well-studied paradigm of imprinting regulation. *Igf2* encodes a potent foetal growth factor and mice that lack the gene are only 50-60% of normal size at birth (DeChiara et al., 1991). *H19* encodes an RNA of uncertain function (Hao et al., 1993; Jones et al., 1998; Li et al., 1998). Both genes are expressed coordinately in the majority of foetal tissues that arise from endodermal and mesodermal lineages.

Several elements have been identified that are important for the coordinate regulation of imprinting and expression of *Igf2* and *H19*. A set of two endodermal enhancer elements are located a few kilobases downstream of *H19*, and are necessary for endodermal expression of both genes (Leighton et al., 1995a). The access of the *Igf2* promoters to these enhancers is restricted on the maternal allele by a chromatin boundary element located upstream of *H19* (Bell and Felsenfeld, 2000; Hark et al., 2000; Kaffer et al., 2000; Kanduri et al., 2000; Szabo et al., 2000; Thorvaldsen et al., 1998). On the paternal allele, *H19* is silenced by promoter methylation (Bartolomei et al., 1993; Ferguson-Smith et al., 1993). The intergenic region and the region upstream of *Igf2* contain silencer elements that are also crucial for keeping the maternal *Igf2* gene silenced (Ainscough et al., 2000a; Constancia et al., 2000). The silencer

upstream of *Igf2*, like the chromatin boundary upstream of *H19*, is epigenetically regulated by DNA methylation (Eden et al., 2001; Holmgren et al., 2001).

However, a complete picture of *Igf2* and *H19* regulation and their phenotypic effects has not emerged, partly because some of the crucial elements have yet to be identified. The *Igf2* silencers show specificity for mesodermal tissues (Ainscough et al., 2000a; Constancia et al., 2000); it is unknown whether there are similar elements for endodermal tissues. What is clear, however, is that several mesodermal enhancers must exist for *Igf2* and *H19*. One of these is located on a YAC transgene that extends to 35 kilobases downstream of *H19* (Ainscough et al., 2000b) and is likely to be downstream of the endoderm enhancers (Kaffer et al., 2000). Several conserved sequence elements have been detected in this region, some of which can direct expression in some mesodermal tissues in transgenic assays (Ishihara et al., 2000). Other mesodermal elements are outside the region covered by the YAC transgene (Ainscough et al., 2000b).

We show that the radiation-induced mouse mutation minute (*Mnt*) (Cattanach et al., 2000) has lost expression of *Igf2* in mesodermal tissues and in the placenta, thus leading to intrauterine growth retardation. The molecular identification of the mutation enabled us to locate mesodermal and extra-embryonic enhancers that are required for *Igf2* expression, and has provided a valuable mouse model for complex regulatory mechanisms in imprinted gene clusters.

MATERIALS AND METHODS

Growth analysis

Crosses were set up between different strains of mice as required, and vaginal plugs were checked daily. For developmental staging purposes, the day of vaginal plug detection is considered to be day 1 of pregnancy. The days of embryonic development (E) were counted from day 1. The days of postnatal development (P) were counted from day 1 being the day of birth. In all experiments the wet weight of embryos, placentae and other organs are the weights after partial removal of fluid from around the tissue with absorbent paper. An unbalanced analysis of variance (Genstat statistical package) was used to test for differences between the genotypes (wild type and mutant), taking into account differences between litters. The tables of means were derived by calculating the mean of the mean weights of individual offspring of the genotype concerned in each litter. This provides a more representative analysis, accounting for the differing number of mutant and wild-type animals in each litter, and minimising the variation that could occur due to environmental differences that individual litters might have experienced. The standard deviation (s.d.) was obtained using the standard formula for the variants of the mean of random variables:

$$\sqrt{\left[\frac{(\text{s.d.}_1)^2 + (\text{s.d.}_2)^2 + (\text{s.d.}_n)^2 \ldots.}{n}\right]}$$

where s.d._1 was the s.d. for litter 1 etc. and n was the number of litters.

Mouse strains used

The mice used in most experiments (and controls) were F_1 hybrids from C57BL/6J and CBA/Ca inbred strains, which are of *Mus musculus* domesticus origin.

SD7 is a congenic stock in which the distal region of chromosome 7 is of *Mus spretus* origin on an otherwise *Mus musculus domesticus* background. It was produced by backcrossing mice carrying the *Mus spretus Igf2-H19* region to the F_1 hybrid C57BL/6J×CBA/Ca background over four generations and then intercrossing these to make homozygotes.

The minute mutation (*Mnt*) investigated was induced in a male mouse of an F_1 (C3H/HeH×101/H) hybrid background. It was subsequently crossed with SD7 and F_1 (C57BL/6J×CBA/Ca) hybrid stock to produce SD7/*Mnt* and F_1/*Mnt* animals respectively, although the region surrounding the *Mnt* mutation is assumed to retain its C3H/HeH or 101/H genetic identity.

Igf2 RIA

Radioimmunoassay for Igf2 was performed on mouse serum as previously described (Hill, 1990) after extraction of Igf2 binding proteins by separation on Sephadex G50. Cross-reactivity of Igf1 in the Igf2 RIA was less than 2%.

Nothern blot analysis

RNA was extracted from tissues using a Qiagen RNeasy Kit according to the protocol of the manufacturer. The concentration and purity of RNA was determined by measuring the absorbance at 260 nm and 280 nm in a spectrophotometer (Cecil 2041). RNA (10 μg) was electrophoresed through 1% formaldehyde gels and subsequently blotted onto nylon membrane according to the protocol supplied (Schleicher and Schuell). The filters were hybridised with DNA probes labelled with [α-^{32}P]dCTP using Pharmacia's oligolabelling kit and the random priming method (Feinberg and Vogelstein, 1983). Prehybridisations and hybridisations were performed in hybridisation buffer (0.5 M sodium phosphate, pH 7.2, 1 mM EDTA, 7% SDS) at 65°C. After hybridisation, the filters were washed in 25 mM sodium phosphate, pH 7.2, 1% SDS at 65°C, and exposed to X ray film for an appropriate length of time. The probes used were as follows: a 0.9 kb *Kpn*I/*Bam*HI genomic fragment which detects all *Igf2* transcripts, comprising intron 5 and the 5′ region of exon 6 (Feil et al., 1994). A 2.2 kb *Eco*RI/*Bam*HI fragment that specifically detects the P0 transcript of *Igf2* (Moore et al., 1997). A 1.9 kb *Eco*RI fragment comprising the entire *H19* cDNA sequence, and a 250 bp *Hin*dIII/*Pst*I fragment comprising the 5′ end of the glyceraldehyde-3-phosphate dehydrogenase gene (*Gapdh*) for RNA loading control.

RT-PCR

First strand cDNA synthesis from 1 μg of total RNA was performed using GibcoBRL Superscript II Reverse Transcriptase according to the protocol of the manufacturer using random hexamers as primers. *Igf2* PCR was performed on the cDNA, using primers GGCCCCGGAGAGACTCTTGC (forward) and TGGGGGTGG-GTAAGGAGAAAC (reverse) (60°C annealing temperature, 2.5 mM $MgCl_2$). PCR products were digested with *Bsa*AI in order to determine the allelic origin of the transcript (Dean et al., 1998).

In situ hybridisation

E14 embryos were fixed for 3-4 hours at 4°C in Bouins solution (75 ml picric acid, 25 ml 37% formalin, 5 ml glacial acetic acid), wax embedded and sectioned at 7 μm. Sections were post-fixed in 4% paraformaldehyde (PFA) in PBS and subjected to in situ hybridisation according to published protocol (Braissant and Wahli, 1998). A 426 bp *Bam*HI/*Sac*I fragment from mouse *Igf2* cDNA (encompassing exon 5) was used to generate sense and antisense probes to detect the *Igf2* transcripts. The probes were labelled by in vitro transcription using the digoxigenin RNA labelling kit (Roche) and NBT/BCIP was used to detect the signal in accordance with the manufacturer's protocol.

Genotyping by PCR

Genomic DNA was prepared according to a standard protocol (Laird et al., 1991). PCR using the following primer combinations (56°C annealing temperature) was used to identify wild-type and *Mnt* samples: GGTTCCTGCCTTGAGTCCTTA (forward) and TTTGGGTGGCTAAGTGCTCAG (reverse) amplify over BP2 on the

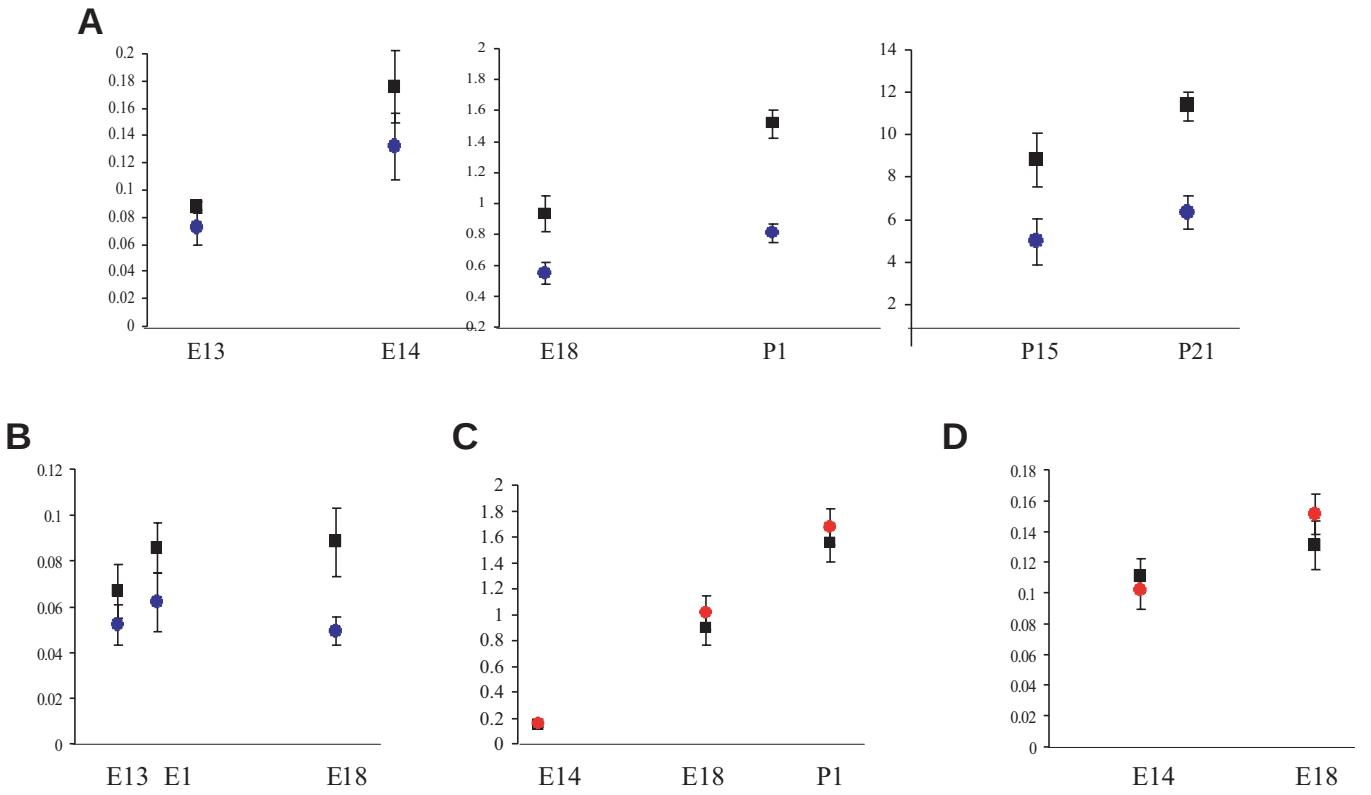

Fig. 1. Foetal and placental weights of *Mnt* mutants. Weights following paternal (blue circles) and maternal (red circles) transmission of the *Mnt* mutation, and their corresponding wild-type littermates (black squares) are shown in grams. (A) Foetal weights at embryonic (E) and postnatal (P) stages following paternal transmission of the *Mnt* mutation. (B) Placental weights with paternal transmission of *Mnt* (blue circles). (C) Foetal weights at embryonic (E) and postnatal (P) stages following maternal transmission of the *Mnt* mutation. (D) Placental weights with maternal transmission of *Mnt* (red circles).

Mnt chromosome (Fig. 6D); CACAGCCCTCAAACCCACTAA (forward) and GGGCAGTAGAGGAGCAAGCAT (reverse) amplify over BP1 on the wild-type chromosome. PCR primers CGTGTGAAGGCACACCTG (forward) and GAGCATCTGTGTGT-GTGCCT (reverse) were used to amplify a polymorphism at MIT marker D7Mit167 to determine the presence of either an SD7 (219 bp product) or Domesticus (189 bp product) allele.

Southern hybridisation

Genomic DNA digested with the appropriate enzymes was electrophoresed through a 1×TBE-agarose gel of appropriate concentration and subsequently immobilised on nylon membrane (Schleicher and Schuell) according to the protocol supplied with the membrane using 0.4 M NaOH. After the transfer of DNA, the filters were neutralised in 1.5 M NaCl, 0.5 M Tris (pH 8) before hybridisation. The filters were hybridised with [α-^{32}P]dCTP-labelled DNA probes as described above. Before hybridisation, labelled cosmids were incubated with 250 μg of sheared genomic DNA for 1 hour at 65°C to block hybridisation to repetitive DNA sequences.

FISH

Fluorescent in situ hybridisation (FISH) was performed essentially as described (Croft et al., 1999) on three-dimensionally preserved nuclei using adult spleen cells from a heterozygous *Mnt* mouse applied to poly-L-lysine slides at a density of approximately 5×10^4/cm^2 and treated before hybridisation as described (Croft et al., 1999). Cosmid AH (Fig. 5) and a BAC-spanning BP2 were labelled with biotin and digoxigenin, respectively, using the Nick Translation System (Promega). Probes (30-50 ng per slide) were precipitated with 10 μg of *Cot*I DNA and 5 μg of salmon sperm DNA and re-suspended in 10 μl of hybridisation mix (50% deionised formamide, 2×SSC, 1% Tween, 10% dextran sulphate). Before hybridisation, the probe

Table 1. Foetal and postnatal weights following transmission of *Mnt* mutation

Genotype	Age	Weight in g (±s.d.)	Offspring: litters	Difference in mean weights (%)
Pat+	E13	0.087±0.004	16:3	83.2**
Mnt^P	E13	0.073±0.013	18:3	
Pat+	E14	0.175±0.027	15:4	75.2**
Mnt^P	E14	0.132±0.024	15:4	
Pat+	E18	0.933±0.117	14:3	59.1**
Mnt^P	E18	0.551±0.072	15:3	
Pat+	P1	1.513±0.092	18:3	53.3**
Mnt^P	P1	0.807±0.061	6:3	
Pat+	P15	8.802±1.298	47:4	56.3**
Mnt^P	P15	4.960±1.110	19:4	
Pat+	P21	11.336±0.689	26:5	55.8**
Mnt^P	P21	6.332±0.797	7:5	
Mat+	E14	0.149±0.019	16:5	108.7 (NS)
Mnt^M	E14	0.162±0.009	17:5	
Mat+	E18	0.894±0.132	22:4	113.6*
Mnt^M	E18	1.016±0.098	16:4	
Mat+	P1	1.553±0.148	16:4	107.7*
Mnt^M	P1	1.674±0.137	14:4	

The significance values were obtained from unbalanced analysis of variance: NS not significant; *P<0.01; **P<0.001. E, embryonic; P, postnatal.

Table 2. Placental weights following transmission of *Mnt* mutation

Genotype	Age	Weight in g (±s.d.)	Offspring: litters	Difference in mean weights (%)
Pat+	E13	0.067±0.012	15:3	78.0**
Mnt^P	E13	0.052±0.009	17:3	
Pat+	E14	0.086±0.011	15:4	72.6**
Mnt^P	E14	0.063±0.013	15:4	
Pat+	E18	0.088±0.015	14:3	55.9**
Mnt^P	E18	0.049±0.006	15:3	
Mat+	E14	0.111±0.111	16:5	91.9 (NS)
Mnt^M	E14	0.102±0.012	17:5	
Mat+	E18	0.131±0.016	22:4	115.3*
Mnt^M	E18	0.151±0.013	16:4	

The significance values were obtained from unbalanced analysis of variance: NS, not significant; *P<0.01; **P<0.001.

hybridisation mix was denatured at 70°C for 5 minutes and pre-annealed at 37°C for 15 minutes. Hybridisation was performed for 36 hours at 37°C in a dark moistened chamber. After hybridisation, slides were washed four times for 3 minutes in 50% formamide/2×SSC, pH 7.5 at 45°C, four times for 3 minutes in 2×SSC at 45°C, four times for 3 minutes in 0.1×SSC 60°C and transferred to 4×SSC/0.1% Tween 20 (Solution A). Blocking buffer (40 μl 4×SSC/5% Marvel) was applied for 5 minutes prior to application of the first antibody. Each antibody incubation was performed in a dark moistened chamber for 1 hour at 37°C. Slides were washed three time for 3 minutes with Solution A at 37°C in between each antibody incubation. Antibodies were diluted in blocking buffer and applied in the following order: sheep anti-digoxigenin (1:1000), rabbit anti-sheep fluorescein (1:200), goat anti-rabbit fluorescein (1:200) and avidin D-Texas Red (1:250) together, goat anti-avidin D-Biotin (1:250), and D-Texas Red (1:250).

Production of transgenic mice and β-galactosidase staining

DNA fragments to be injected were liberated from vector sequences by restriction digestion, electrophoresed in an agarose gel and recovered using QIAEX II gel extraction kit (Qiagen). Fertilised one-cell eggs were microinjected with about 200 copies of the transgene fragments, cultured overnight and transferred to the oviducts of pseudopregnant females at the two-cell stage. Embryos were recovered at E14 and fresh frozen, while the yolk sacs were collected and stained for β-galactosidase activity as described (Hogan et al., 1994) in order to identify embryos that expressed the transgene. Positive embryos were subsequently cryosectioned at a thickness of 15 μm and slides were processed for β-galactosidase activity according to the above method.

RESULTS

Altered foetal growth correlates with levels of *Igf2* expression

Paternal transmission of the *Mnt* (Mnt^P) mutation resulted in intrauterine growth retardation (IUGR) first detected at E13 with a birth weight of >50% of normal (Cattanach et al., 2000). Placental weights were also reduced, and there were postnatal losses of up to 75% of the Mnt^P offspring between birth and weaning, the extent of which was strongly dependent on genetic background. Homozygous *Mnt* foetuses died between E15 and E17 (Cattanach et al., 2000).

Progeny from paternal transmission of the *Mnt* mutation [F_1 C57BL/6J×CBA/Ca) female × (F1/*Mnt*) male] and maternal transmission (*Mnt*/SD7 female×SD7 male) were collected at various time points and the wet weights were analysed. The statistical significance between the weights of wild-type (+) and *Mnt* littermates was determined by an unbalanced analysis of variance test, performed using the linear model fitting facilities of the Genstat statistical package (see Materials and Methods for details).

The growth retardation resulting from paternal transmission of *Mnt* was evident at embryonic (E) day 13 (83% of +), although the difference between + and Mnt^P littermates increased until the day of birth (53% of +) (Fig. 1A, Table 1). Placental weights were also reduced from E13 (78% of +), reaching 56% of + at E18 (Fig. 1B, Table 2). The size difference between + and Mnt^P offspring observed at birth averaged 55%, but can vary depending on the genetic background (the inheritance of an SD7 allele appears to affect birth weights – data not shown) and was subsequently maintained into adulthood (Fig. 1A, Table 1). While in E18 litters the expected 50% of Mnt^P offspring was observed, there were immediate postnatal losses of Mnt^P animals so that on the day of birth (P1) only one third of the expected Mnt^P offspring were present (Table 1). The cause of death is currently not known.

Maternal inheritance of the *Mnt* mutation (Mnt^M) resulted in

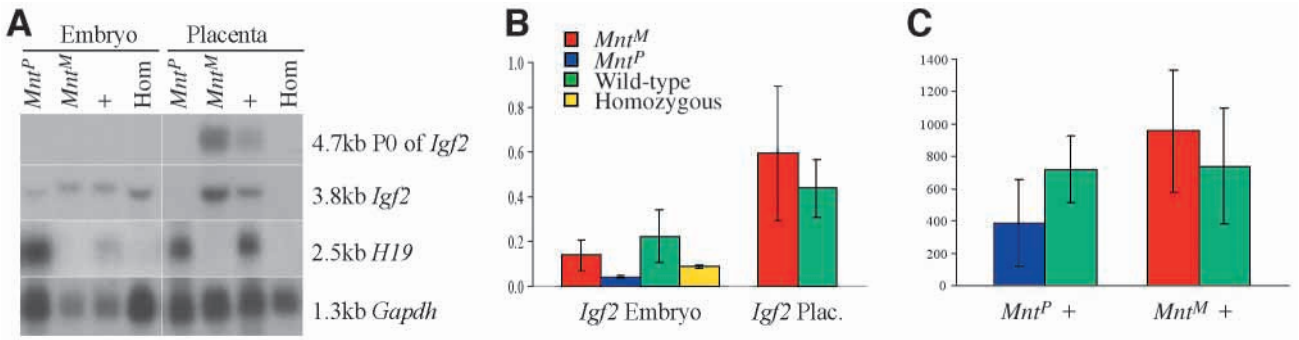

Fig. 2. Expression analysis of *Igf2* and *H19* in *Mnt*. (A) Northern blot analysis of total RNA prepared from the different classes of E14 intercross embryo and placenta samples; Mnt^P n=4; Mnt^M n=4; wild type n=4; homozygous *Mnt* (Hom) n=2 (n=sample number analysed). (B) Histogram of *Igf2* (3.8 kb transcript) relative expression levels obtained in A normalised against *Gapdh* for each class of intercross sample, error bars show the standard deviations. (C) Circulating Igf2 serum (ng/ml) levels in neonates (P1) following paternal (n=12) and maternal (n=17) transmission of *Mnt*, and their corresponding wild-type littermates (n=9 and n=11, respectively). Error bars show the standard deviations.

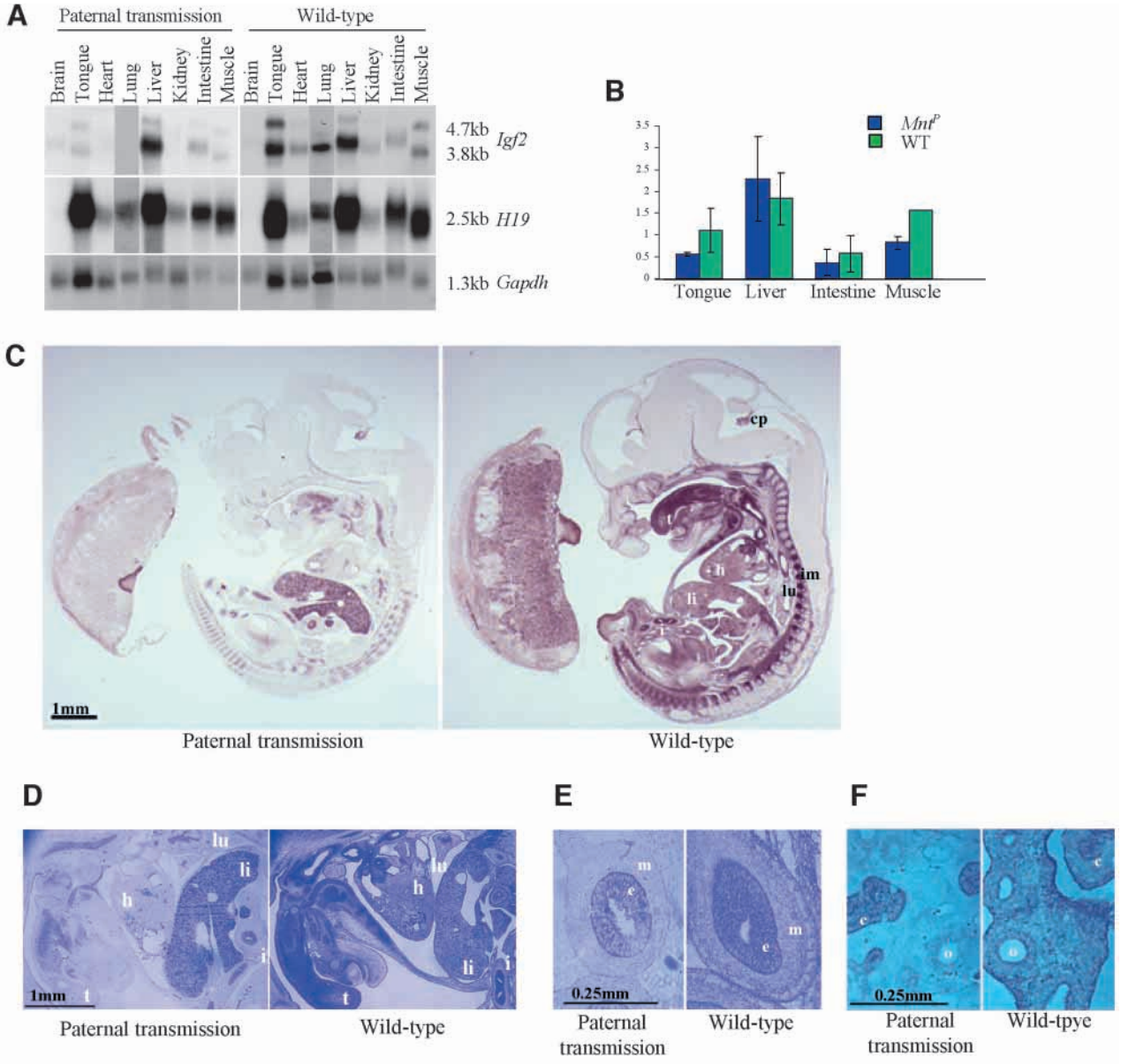

Fig. 3. Tissue specific analysis of *Igf2* expression. (A) Northern analysis of *Igf2* and *H19* in neonatal (P1) tissues following paternal transmission of *Mnt* and the corresponding wild-type littermates. (B) Histogram of relative *Igf2* expression levels normalised against *Gapdh*. Error bars show the standard deviations when multiple samples were analysed: tongue 35% (n=2 wild type, n=2 Mnt^P), liver 110% (n=5 wild type, n=6 Mnt^P), intestine 71% (n=4 wild type, n=5 Mnt^P), muscle 62%% (n=1 wild type, n=2 Mnt^P). (C) In situ hybridisation analysis of *Igf2* expression in E14 Mnt^P embryos and placentae. Images were captured with standardised exposure times, degree of illumination and level of magnification. Choroid plexus (cp), tongue (t), heart (h), lung (lu), liver (li), intestine (i) and intercostal muscle (im). Note the difference in embryonic and placental sizes between Mnt^P and wild type. (D) Higher magnification of some organs. Note the reduced levels (apparently cell-type specific) observed in the intestine, lung and tongue. (E) Cell-type specific expression within the intestine. Expression in Mnt^P is retained in the endodermal epithelial lining (e) but lost in the mesodermal muscular layer (m) of the intestine. (F) Cell-type specific expression within the lung. *Igf2* expression in Mnt^P is only retained in those bronchi with closed lumen (c) while it is lost in the open bronchi (o) and mesenchyme.

foetal overgrowth, which was first significant at E18 (113% of +, Fig. 1C, Table 1). Overgrowth (108% of + on the day of birth) did not affect survival and equal numbers Mnt^M and + neonates were obtained. Similarly, maternal transmission of *Mnt* resulted in an overgrown placenta on E18 (115% of +) (Fig. 1D, Table 2). This effect of maternal transmission of the mutation on growth has not previously been described (Cattanach et al., 2000), presumably because the effect is only moderate.

Paternal transmission of *Mnt* thus resembled the phenotype of *Igf2*-null mice (DeChiara et al., 1991), whereas maternal transmission resembled that of the *H19* knockout, which expresses *Igf2* biallelically (Leighton et al., 1995b), although here the degree of overgrowth is not as great. As *Mnt* was genetically linked to MIT markers D7Mit46 and Mit167 (Cattanach et al., 2000) located at the *Igf2* gene on distal chromosome 7, expression levels of *Igf2* were analysed by northern blotting to determine if the growth phenotype was

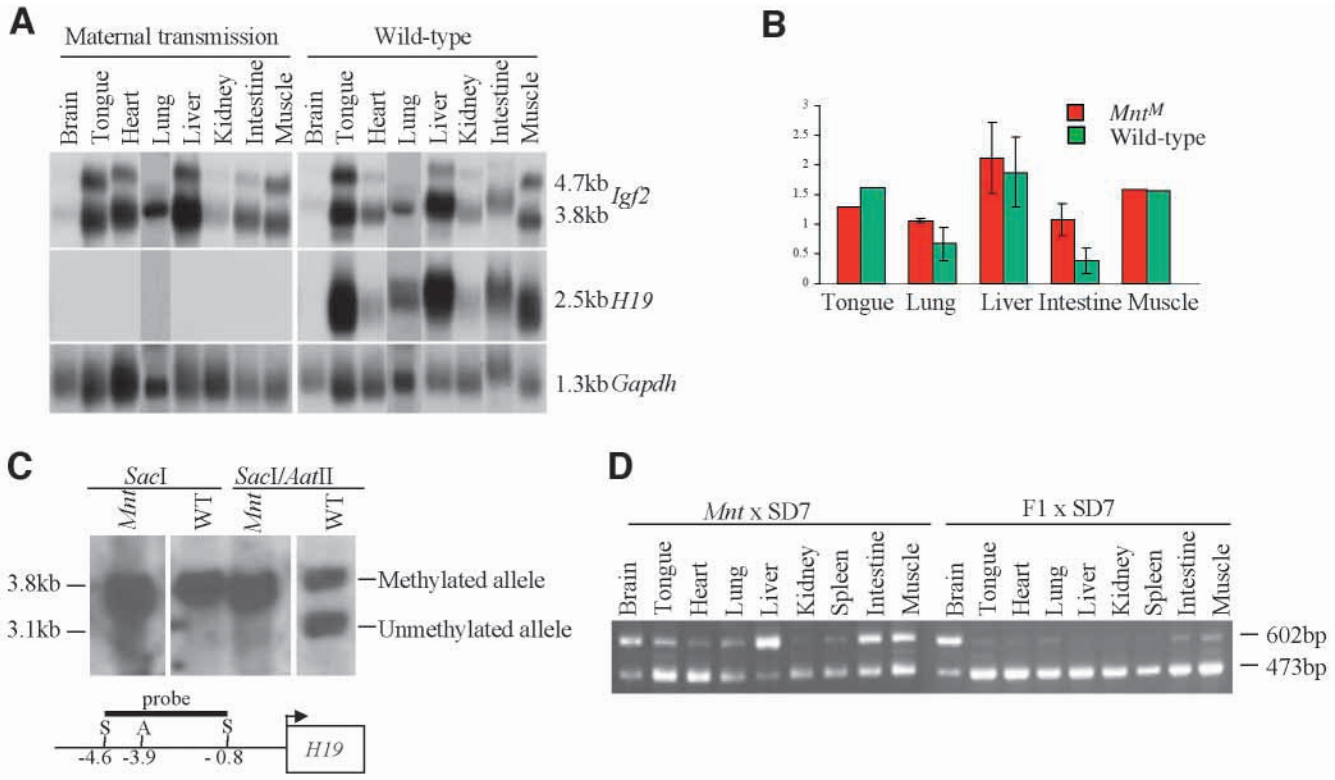

Fig. 4. Expression and methylation analysis with maternal transmission of *Mnt*. (A) Northern analysis of *Igf2* and *H19* in neonatal (P1) in Mnt^M and the corresponding wild-type littermates. (B) Representation of the *Igf2* expression levels normalised against *Gapdh* (in tissues in which *Igf2* expression was detectable after paternal transmission). Error bars show the standard deviations when multiple samples have been analysed. Tongue wild type n=1, Mnt^M n=1; lung wild type n=4, Mnt^M n=3; liver wild type n=5, Mnt^M n=3; intestine wild type n=4, Mnt^M n=4; muscle wild type n=1, Mnt^M n=1. (C) Methylation analysis of *H19* DMR in homozygous *Mnt* foetuses (E17) using a 3.8 kb *Sac*I probe, hybridised to *Sac*I- and *Aat*II-(methylation sensitive) digested genomic DNA (Tremblay et al., 1995). Note the absence of the unmethylated allele in the homozygous *Mnt* sample, showing methylation of the maternal *Mnt* allele, while in the wild type the maternal allele is unmethylated. (D) Allele specific expression analysis of *Igf2* in Mnt^M neonatal (P1) tissues (*Mnt*×SD7) and the corresponding wild-type littermates (F_1×SD7) by RT-PCR (Dean et al., 1998) (three individual samples analysed). The 602 bp band corresponds to the maternal allele, while the 473 bp corresponds to the paternal SD7 allele.

induced through alterations in the control of *Igf2*. Embryos were obtained from (*Mnt*/SD7) female × (F1/*Mnt*) male intercrosses at E14, before the death of homozygous *Mnt* embryos (Fig. 2A). This cross allowed the distinction of the parental origin of the different alleles and all four classes of embryos were obtained (verified by genotyping PCR – see Materials and Methods for details), although homozygous embryos were under-represented (from nine litters + (SD7/F1) n=16; Mnt^M (*Mnt*/F1), n=18; Mnt^P (SD7/*Mnt*), n=23; *Mnt/Mnt*, n=4). Homozygous embryos did not significantly differ in weight from Mnt^P embryos at E14 (data not shown), although their placentae were smaller [homozygous placenta were 60% of + (data not shown) compared with 78% of + for Mnt^P at E14].

Igf2 expression was substantially reduced in Mnt^P embryos (18% of +) and in homozygous *Mnt* embryos (38% of +), but was normal in Mnt^M embryos at this stage (Fig. 2A,B). *Igf2* transcripts, including the placenta-specific transcript P0, were absent from the placenta of Mnt^P and homozygous *Mnt* embryos (Fig. 2A,B). Moreover, the neighbouring maternally expressed *H19* gene was silenced in both Mnt^M and homozygous *Mnt* embryos and placentae, while paternal transmission of the mutation did not affect its expression (Fig. 2A).

Additionally, serum levels of Igf2 peptide were determined in Mnt^M and Mnt^P neonates (Fig. 2C). Circulating levels of Igf2 were reduced in Mnt^P mice (54% of +), and were elevated in the Mnt^M mice (129% of +). Thus, there is a correlation between the levels of *Igf2* transcripts, the levels of circulating Igf2 peptide, and the growth patterns observed in the two classes of *Mnt* mutants (maternal and paternal transmission) in comparison to + animals. Thus, the *Mnt* mutation is highly unusual in that three different classes of phenotype are observed: IUGR following paternal transmission, overgrowth after maternal transmission, and embryonic lethality in the homozygous state.

Paternal transmission of *Mnt* leads to repression of *Igf2* in mesodermal tissues and placenta

The northern blot analysis of whole foetuses showed that while the level of *Igf2* expression was substantially reduced in E14 Mnt^P embryos (Fig. 2), some residual levels of expression remained (18%). Therefore, *Igf2* transcripts were analysed in specific tissues from Mnt^P neonates (Fig. 3A). A striking pattern of tissue specificity was found, with complete repression of *Igf2* in the heart, lung and kidney, substantially reduced levels of *Igf2* in the tongue and skeletal muscle (35%

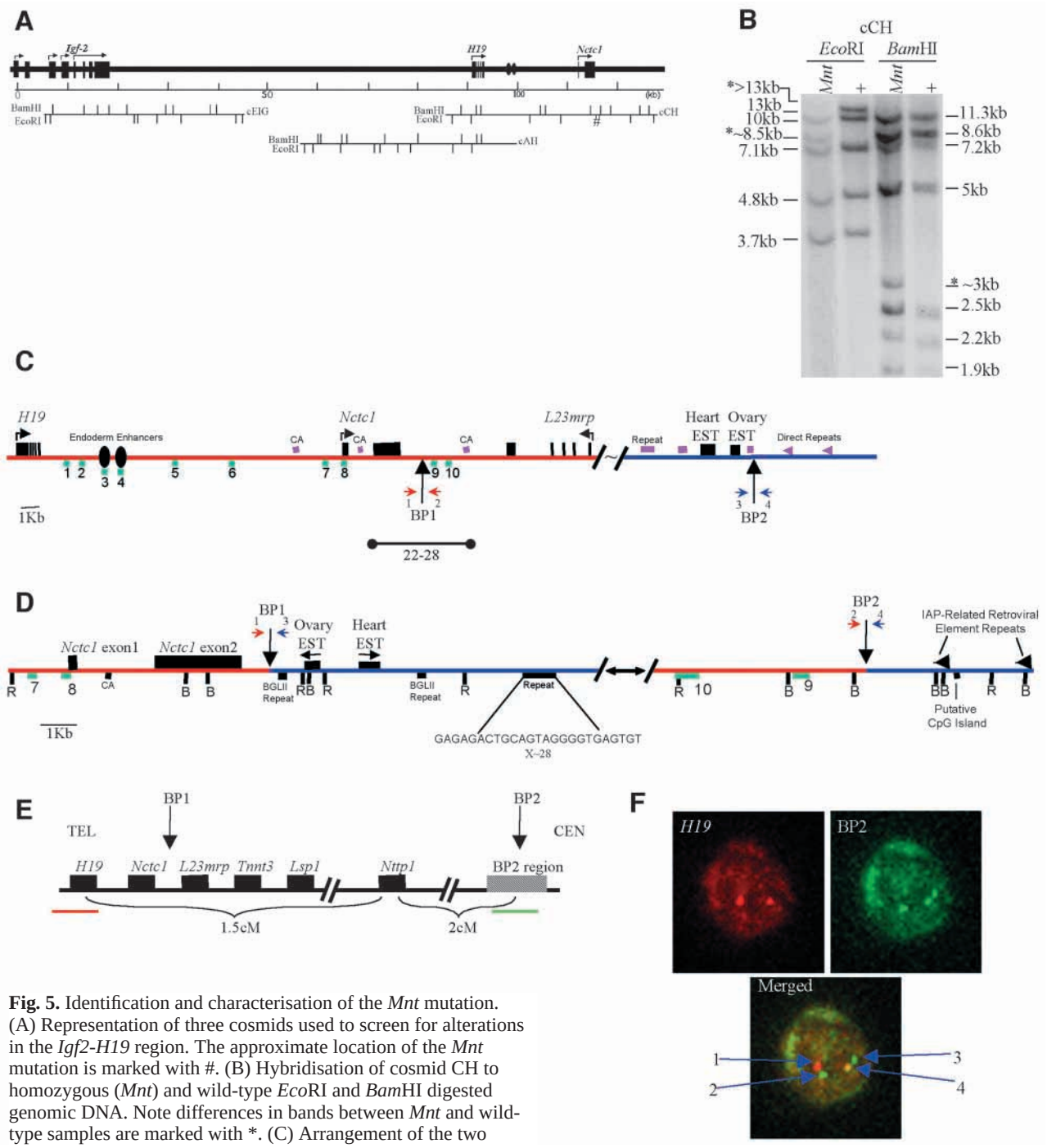

Fig. 5. Identification and characterisation of the *Mnt* mutation. (A) Representation of three cosmids used to screen for alterations in the *Igf2-H19* region. The approximate location of the *Mnt* mutation is marked with #. (B) Hybridisation of cosmid CH to homozygous (*Mnt*) and wild-type *Eco*RI and *Bam*HI digested genomic DNA. Note differences in bands between *Mnt* and wild-type samples are marked with *. (C) Arrangement of the two breakpoint regions on a wild-type chromosome. The breakpoint 1 (BP1) region (downstream of *H19*) is shown as a red line, while the BP2 region which is 3.5 cM further centromeric is shown as a blue line. The regions conserved between mouse and human (1-10) as identified by Ishihara et al. (Ishihara et al., 2000) are shown (green squares), while the region (+22 to +28 kb from the *H19* promoter) identified by Kaffer et al. (Kaffer et al., 2000) as possessing enhancer activity is shown by a black line. (D) The arrangement of the two breakpoint regions on the *Mnt* chromosome. Note that the rearrangement isolates the conserved elements 9 and 10 from the *H19* region. PCR primers (1-4) for the detection of the breakpoints are shown. (E) Relative positions of the two *Mnt* breakpoints, the surrounding genes and the genetic distance between the two breakpoints. The red and green lines represent the probes used in the FISH analysis. (F) Fluorescence in situ hybridisation (FISH) analysis on heterozygous *Mnt*/F1 nuclei, verifying that an inversion has occurred on the *Mnt* chromosome. Red, *H19* probe; green, BP2 probe. In the merged image, 1 is the *H19* region on the wild-type chromosome; 2 is the BP2 region on the wild-type chromosome; 3 is the 3′ part of the BP2 region on the *Mnt* chromosome (see E); and 4 is the co-localisation of the 5′ part of the BP2 region and the *H19* region on the *Mnt* chromosome (yellow).

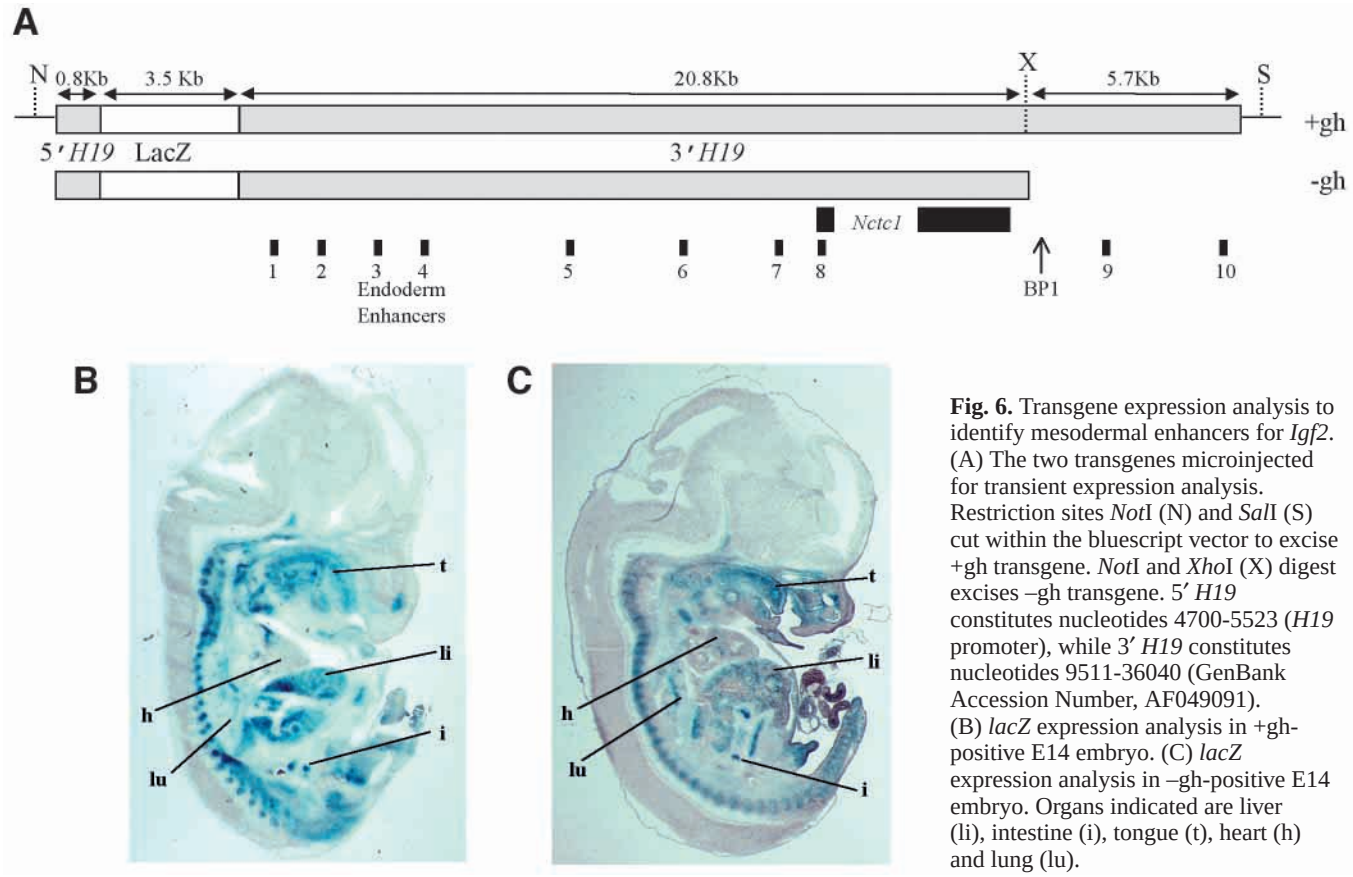

Fig. 6. Transgene expression analysis to identify mesodermal enhancers for *Igf2*. (A) The two transgenes microinjected for transient expression analysis. Restriction sites *Not*I (N) and *Sal*I (S) cut within the bluescript vector to excise +gh transgene. *Not*I and *Xho*I (X) digest excises –gh transgene. 5′ *H19* constitutes nucleotides 4700-5523 (*H19* promoter), while 3′ *H19* constitutes nucleotides 9511-36040 (GenBank Accession Number, AF049091). (B) *lacZ* expression analysis in +gh-positive E14 embryo. (C) *lacZ* expression analysis in –gh-positive E14 embryo. Organs indicated are liver (li), intestine (i), tongue (t), heart (h) and lung (lu).

and 62%, of + respectively), and moderately reduced levels in intestine (71%). By contrast, *Igf2* expression levels in the neonatal liver (and E14 livers – data not shown) were normal, although variations were observed (Fig. 3A,B). Reduction of *Igf2* expression was therefore found in all organs with mesodermal tissue contributions.

The distribution of *Igf2* expression was further analysed in detail by in situ hybridisation. This confirmed that *Igf2* expression was abolished in the placenta (Fig. 2; Fig. 3C) and in mesodermal tissues such as the heart and kidney. Expression in other mesodermal tissues (intercostal muscle and tongue) was greatly reduced (Fig. 3C,D). Importantly, in tissues that possess both endodermal and mesodermal components (e.g. intestine), the residual *Igf2* expression was restricted to the epithelial lining (endodermal) and expression was absent in the smooth muscle (mesodermal) layer (Fig. 3D,E) thus explaining the partial reduction of *Igf2* levels on northern blots. This pattern of expression was also observed in the lung where *Igf2* was downregulated in the mesenchymal tissues, but continued to be expressed from the epithelial cells in the bronchi (Fig. 3F). However, there was heterogeneity in that bronchi with no or small lumina continued to express *Igf2*, but those with a larger lumen did not (Fig. 3F). Whether this indicates a developmental delay of the *Mnt* lung, or heterogeneity of *Igf2* regulation during development of the bronchial epithelium is not known. Other notable regions that lack *Igf2* expression in the Mnt^P embryo include the dermal layer, diaphragm and genital tubercle. It is interesting to note that the choroid plexus, a tissue that normally expresses *Igf2* biallelically (DeChiara et al., 1991), maintained normal levels of *Igf2* expression in Mnt^P embryos (Fig. 3C). Hence, the regulatory elements that control *Igf2* expression in this tissue are not disrupted by the *Mnt* mutation.

We conclude that the presence of the *Mnt* mutation on the paternal allele results in a disruption of *Igf2* expression specifically in mesodermal tissues. This could occur as a result of the disruption of regulatory elements required for *Igf2* expression in mesodermal tissues such as enhancers. The pattern of residual *Igf2* expression is indeed largely complementary to that in the knockout of the endodermal enhancers for *Igf2* (Leighton et al., 1995a).

Maternal transmission of *Mnt* leads to methylation and repression of *H19*

Analysis of the expression patterns of *Igf2* and *H19* following maternal transmission of the *Mnt* mutation demonstrated that *H19* was repressed in all neonatal tissues analysed (Fig. 4A). This was associated with aberrant DNA methylation of the maternal *H19* allele in the DMR upstream of *H19* (Fig. 4C) and in the *H19* promoter (not shown) in all stages and tissues analysed. (Paternal transmission of *Mnt* did not lead to altered methylation of the *H19* DMR, which remained methylated.) *Igf2* transcript levels by contrast were elevated in lung, liver and intestine (Fig. 4A,B) after maternal transmission of the *Mnt* mutation. As the endodermal enhancers are likely to be intact in Mnt^M (ascertained from the analysis of Mnt^P animals), methylation of the DMR boundary region upstream of *H19* might lead to reactivation of the maternal allele of *Igf2* in endodermal tissues. Allele specific expression analysis of *Igf2* using RT-PCR did indeed reveal that the maternal *Igf2* allele

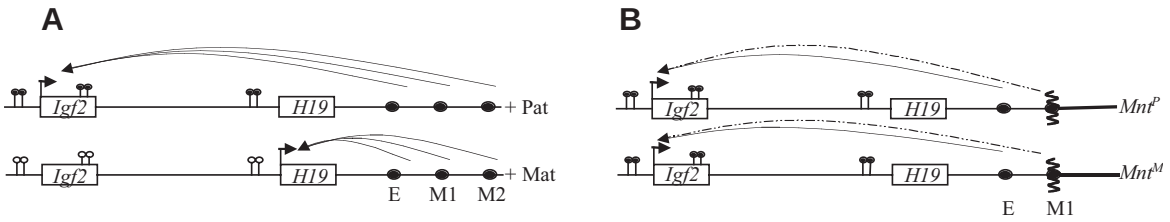

Fig. 7. Summary of the main features of the *Mnt* mutation. (A) The situation in wild type with the endoderm enhancers (E), the mesoderm enhancers for tongue and skeletal muscle (M1), and the mesodermal enhancers for heart, lung and kidney (M2) activating paternal *Igf2* and maternal *H19*. (B) The *Mnt* situation with disruption of the M1 enhancers, isolation of the M2 enhancers, maternal methylation at the *H19* DMR (hence the absence of a functional boundary on the maternal allele), absence of *H19* expression, and subsequent biallelic activation of *Igf2* from the remaining active enhancers (E).

was expressed in liver, lung and intestine of Mnt^M animals (Fig. 4D), which thus accounts for the increased levels of expression of *Igf2* (Fig. 4A), and the increased Igf2 serum levels (Fig. 2). In addition, the activation of *Igf2* from the maternal Mnt^M allele in endodermal tissues can account for the higher levels of *Igf2* expression observed in homozygous *Mnt* embryos compared with Mnt^P heterozygotes (Fig. 2).

The *Mnt* mutation is an inversion that disrupts a candidate region for muscle specific enhancers

The *Mnt* mutation was induced using radiation mutagenesis, a technique that often results in rearrangements (translocations, inversions, insertions or deletions) (Cattanach et al., 1993). Cytogenetic analysis by G-banding, however, provided no evidence of any gross chromosomal changes in *Mnt* (Cattanach et al., 2000).

In order to identify any minor chromosomal change, a 130 kb region encompassing 5′ of *Igf2* to 3′ of *H19* was analysed in detail by Southern hybridisation with 3 cosmids (Fig. 5A). The cosmids were hybridised to *Eco*RI- and *Bam*HI-digested genomic DNA from homozygous *Mnt* and + embryos. The resulting banding pattern showed that a region covered by cosmid CH had been disrupted in the *Mnt* mutation (Fig. 5B). The expected 13 kb *Eco*RI fragment was replaced by two other fragments (8.5 kb and >13 kb), providing evidence that the *Mnt* mutation was not a deletion (a single fragment has been replaced by two fragments the combined length of which is greater than the original fragment). The appearance of a fragment of a 3 kb was the only abnormality evident in the *Bam*HI digest (Fig. 5B).

The altered 8.5 kb *Eco*RI fragment identified in *Mnt* samples was cloned in a lambda library (Stratagene Lambda FIX II) using homozygous *Mnt* DNA enriched for fragments of approximately 8.5 kb. Clones positive for the expected wild-type sequence 5′ to the region disrupted in *Mnt* were sequenced. The 8.5 kb clone was located approximately 25 kb downstream from the *H19* promoter (Fig. 5, BP1), and approximately 200 bp of novel sequence were found fused to the expected sequence. The 200 bp novel sequence was used to probe a 129/SvJ genomic DNA lambda library (Stratagene catalogue number 946313) and a 16 kb lambda clone was identified that provided the sequence of a second endogenous region (BP2) that was disrupted in *Mnt* (Fig. 5C). This suggested that the *Mnt* mutation was an inversion between two breakpoints (BP1 and BP2). PCR analysis across the breakpoints in the re-arranged DNA confirmed that this was indeed the case (Primers 1 and 3, and primers 2 and 4, Fig. 5D) and that there was no loss of any DNA (Fig. 5D).

The inversion on the *Mnt* chromosome was confirmed by fluorescence in situ hybridisation (FISH) analysis using two probes, one specific for each breakpoint region (Fig. 5E), hybridised to nuclei heterozygous for the *Mnt* mutation (Fig. 5F). Co-localisation of the signal on the *Mnt* chromosome demonstrated that DNA from the BP2 region was relocated close to *H19* on the *Mnt* chromosome (Fig. 5F).

However, this analysis does not provide any indication of the location of the second breakpoint (BP2) (centromeric or telomeric to the BP1 region?), nor does it provide an indication of the distance between the two breakpoints. Genetic mapping using a panel of [*M. m. domesticus* × (*M. m. domesticus* × SD7)] backcross DNAs showed that the BP2 region was approximately 2 cM centromeric of *Nttp1* (two recombinants in 106 meioses occurred between *Nttp1* and BP2) (Fig. 5E). *Nttp1* is located 1.5 cM centromeric of *H19* (Paulsen et al., 1998). Thus, the second breakpoint region is located several megabases (Mb) further centromeric of *H19*.

Sequence analysis of the BP2 region identified several features such as homology to ESTs and repeat structures (Fig. 5C) disruption of which in *Mnt* may contribute to the phenotype. However, because this region is several megabases away from *Igf2* and *H19*, it is unlikely that its disruption causes the altered regulation of the two genes. Instead, we focussed on the analysis of the BP1 region. While this work was in progress, several sequence elements were discovered in the BP1 region that were conserved between mice and humans (Fig. 5C, elements 1-10) (Ishihara et al., 2000). Perhaps of greater significance was that some of these elements displayed enhancer activity. In addition to the known endoderm enhancers (elements 3 and 4), enhancer activity was detected in mesodermally derived structures including embryonic myotome and rib primordia (elements 6 and 9), mesenchymal cells (element 7) and the neural tube floor plate and ectoderm of the limb buds (element 5). Furthermore, in vitro transfection assays confirmed that the region covering approximately +22 to +28 kb from the *H19* promoter possesses enhancer activity in muscle cell lines (Kaffer et al., 2000). The combined evidence indicates that the BP1 region is likely to contain at least one of the long sought mesodermal enhancer regions for *Igf2* and *H19*.

Transgenic identification of mesodermal enhancers

In order to confirm that the BP1 breakpoint region contained

mesodermal enhancers, and that they were affected by the inversion, two transgenic constructs were made (Fig. 6A). The first construct (+gh) contained 0.8 kb 5′ of exon1 of *H19* (the *H19* promoter) coupled to a *lacZ* reporter and a further 27 kb of the region downstream of *H19*. The downstream region contained the 10 regions identified as being conserved between mouse and human. The second construct (–gh) was produced by truncating the first construct at a *Xho*I site located 400 bp upstream of BP1 in *Mnt*, reducing the downstream region to approximately 21 kb (Fig. 6A).

These two transgenes were microinjected into fertilised oocytes and the expression of *lacZ* (driven by the *H19* promoter under the influence of any enhancer elements present on the transgene) was analysed in E14 embryos (Fig. 6). Embryos positive for the +gh transgene showed expression in the liver, epithelial layer of the intestine but not the smooth muscle layer, the epithelial layer of the lung, but not in other cell types in the lung, the tongue, and the cartilage and intercostal muscles. Expression was also absent in the kidney and heart (Fig. 6B). This shows that the enhancers responsible for controlling *Igf2* and *H19* expression in muscle and tongue are present in the BP1 region, while those elements required to drive expression in other mesodermal tissues (heart, kidney and lung) are missing.

The –gh transgene was designed to mimic the *Mnt* mutation, isolating conserved regions 9 and 10 from the rest of the region. The most obvious difference between the two constructs was a reduction in expression levels observed in the tongue and intercostal muscles with construct –gh (Fig. 6C). Expression with the –gh construct continued to be absent in the heart and kidney, and the majority of cell types in the lung (except epithelial cells), while being maintained in the liver and epithelial cells in the intestine (Fig. 6C).

DISCUSSION

This study reports on the molecular characterisation of the *Mnt* mutation, and shows that the mesodermal enhancers controlling expression of *Igf2* in skeletal muscle and tongue are disrupted by this mutation. Furthermore, our results indicate that other mesodermal enhancers that control expression in the heart, lung and kidney, and the placental enhancers are located even further distal to *H19* (Fig. 7), showing that most of the known enhancers are located 3′ of *H19*. Our study also establishes a model in which the effects of *Igf2* deficiency in mesodermal tissues can be studied for the first time. Finally, it reveals that the *H19* maternal germline imprint is either controlled by sequences 3′ to the *Mnt* mutation, or is overridden by novel sequences brought into close proximity to *H19* by the inversion.

Molecular analysis revealed that the *Mnt* mutation is an inversion of a DNA segment encompassing several megabases, which is typical of radiation mutations (Cattanach et al., 1993). Characterisation of the region surrounding the most centromeric breakpoint (BP2) has identified several repeat structures and ESTs. Although the cause of death of the homozygous *Mnt* embryos is not known, the disruption of genes and genetic elements encoded in this region could contribute towards the phenotype. Furthermore, the presence of an inversion and the organisation of the disrupted regions following the rearrangement, could contribute to the characteristics identified in each of the *Mnt* classes. It will be interesting to investigate if expression of any of the adjacent genes (e.g. *Nctc1, L23, Lsp1, Tnnt3*) is also affected by the *Mnt* mutation.

The breakpoint proximal to *H19* (BP1) is in a cluster of DNA elements that show a high degree of conservation between human and mouse (Ishihara et al., 2000). Some of these elements (6,7,9) showed enhancer activity in some mesodermal tissues in transgenic assays. Our analysis shows that the intact cluster is required for appropriate expression of *Igf2* in skeletal muscle and tongue, and suggests cooperation between individual elements is required for full expression in these tissues. Cooperativity of enhancer elements has been shown previously in transgenic mice (Kruse et al., 1995), but not in an in vivo situation such as this. The residual levels of *Igf2* RNA in muscle and tongue may be due to the combination of the remaining elements (5-8). A very recent knockout experiment found that elimination of elements 5-10 resulted in substantial reduction of *Igf2* expression in skeletal muscle and tongue, thus confirming our analysis (Kaffer et al., 2001). The identification of an enhancer for expression in the tongue is of particular relevance to the understanding of the molecular pathology of the human foetal overgrowth syndrome, Beckwith Wiedemannn syndrome, in which overgrowth of the tongue is one of the most consistent symptoms (Maher and Reik, 2000).

The loss of *Igf2* expression in heart, kidney, lung and placenta suggests the additional mesodermal and extra-embryonic enhancer elements are located 3′ to the inversion breakpoint. These elements have thus far not been detected by any transgenic approach (Ainscough et al., 2000b; Kaffer et al., 2000). How far distant they are from the breakpoint is currently not known, but we are sequencing BAC clones covering this area in order to identify conserved segments as candidates for enhancers. Surprisingly, a recent experiment that has placed an additional *H19* DMR 3′ of the endoderm but 5′ of the muscle and tongue enhancers here identified, caused downregulation of *Igf2* expression in the heart by 50% (Kaffer et al., 2001). This may indicate that either the unmethylated chromatin boundary is partially open for the heart enhancers, or that some heart enhancers are not located distal to *H19*, a possibility that is more difficult to reconcile with our results. In *Mnt*, the complete loss of expression in the kidney is surprising, as epithelia, particularly in the glomeruli, would be expected to show expression (the endoderm enhancers are known to be intact and functional in *Mnt*). The endoderm enhancer knockout also showed markedly reduced expression in the kidney (Leighton et al., 1995a), suggesting perhaps again that co-operation between different enhancer elements is required. Expression was found in bronchial epithelia as expected, but not in those with larger lumina, indicating perhaps that as differentiation into secretory epithelia takes place, regions other than the endoderm enhancers are required but are disrupted in *Mnt*.

The location of most known enhancers for *Igf2* distal to *H19* (Fig. 7) now provides an explanation for reactivation of the silent *Igf2* allele in both endodermal and mesodermal tissues when the DMR/boundary region upstream of *H19* is deleted (Leighton et al., 1995b; Thorvaldsen et al., 1998) (Fig. 7). Thus the boundary operates in both tissue types. This leaves unanswered the question of why maternal deletion of silencer

elements in the intergenic region or in DMR1 reactivates the silent *Igf2* allele (Ainscough et al., 2000a; Constancia et al., 2000). It seems most likely now that interaction between these elements might be required for full repression, as previously suggested (Constancia et al., 2000).

A second effect of the *Mnt* mutation is the methylation of the *H19* DMR and associated silencing of the maternal *H19* allele (Fig. 7). This aberrant methlyation leads to reactivation of the maternal *Igf2* allele in all tissues for which enhancers are intact (liver and others) showing for the first time in vivo that the DMR/boundary can be opened by DNA methylation (as well as by deletion). *H19* methylation on the maternal allele is likely to arise in the female germline, or in the early embryo, as it was present in all tissues analysed. It is possible that sequences 3′ to the *Mnt* breakpoint are necessary to keep the maternal *H19* gene unmethylated, although transgenic experiments have shown that sequences further 3′ than 8 kb from *H19* are not necessary for imprinting (Cranston et al., 2001). Alternatively, sequences from the other end of the inversion which have been moved close to *H19* may have a dominant methylating effect. We note particularly in this respect that ovary specific ESTs are located close to the breakpoint with a direction of transcription towards *H19* (Fig. 5D). If there are indeed transcripts running antisense to *H19* and its DMR, this might lead to methylation of the DMR as suggested (Reik and Walter, 1998). The maternal *H19* DMR has also been found to become methylated in some tumours with biallelic *Igf2* transcription (Cui et al., 2001; Nakagawa et al., 2001).

Lack of *Igf2* in many mesodermal tissues and in the placenta leads to intrauterine growth deficiency as expected. However, the magnitude of the effect (as much as in the *Igf2* null) is unexpected as there is normal *Igf2* expression in the liver, leading to substantial serum levels of the peptide. The most likely explanation is that absence of *Igf2* from the placenta leads to marked growth restriction independent of *Igf2* levels in the foetus. Indeed a knockout of the placenta specific *Igf2* transcript resulted in IUGR of 70% of normal birthweight (Constancia et al., 2000). By contrast, overexpression of *Igf2* in the maternal transmission of *Mnt* largely limited to endodermal tissues leads to foetal overgrowth, showing that the contribution of these tissues to circulating Igf2 is substantial.

The molecular analysis of the *Mnt* mutation establishes an important paradigm in genetics in that transmission of the mutation from either parent leads to different phenotypes from wild type, and the homozygous phenotype is different again. A similar (but not identical) pattern of inheritance is seen with the ‘polar overdominance’ mutation *Callipyge* in sheep, in which the phenotype is observed with paternal, but not with maternal transmission or in homozygotes (Charlier et al., 2001). The mutation has not been identified but has recently been linked with abnormal expression of the imprinted gene cluster including *DLK* and *GTL2* (Charlier et al., 2001). We suggest that as in *Mnt* regulatory sequences such as enhancers or silencers in this region might be mutated.

We thank D Brown and E Walters for help with statistical analysis, P. Fraser for advice on FISH, and Ko Ishihara for the construction of the transgenes. We thank all our colleagues for discussion and comments on the manuscript. Our work is supported by BBSRC and HFSP.

REFERENCES

Ainscough, J. F., John, R. M., Barton, S. C. and Surani, M. A. (2000a). A skeletal muscle-specific mouse Igf2 repressor lies 40 kb downstream of the gene. *Development* **127**, 3923-3930.

Ainscough, J. F., Dandolo, L. and Surani, M. A. (2000b). Appropriate expression of the mouse H19 gene utilises three or more distinct enhancer regions spread over more than 130 kb. *Mech. Dev.* **91**, 365-368.

Bartolomei, M. S., Webber, A. L., Brunkow, M. E. and Tilghman, S. M. (1993). Epigenetic mechanisms underlying the imprinting of the mouse H19 gene. *Genes Dev.* **7**, 1663-1673.

Bell, A. C. and Felsenfeld, G. (2000). Methylation of a CTCF-dependent boundary controls imprinted expression of the Igf2 gene. *Nature* **405**, 482-485.

Braissant, O. and Wahli, W. (1998). A simplified in situ hybridisation protocol using non-radioactively labeled probes to detect abundant and rare mRNAs on tissue sections. *Biochemica* **1**, 10-16.

Brannan, C. I. and Bartolomei, M. S. (1999). Mechanisms of genomic imprinting. *Curr. Opin. Genet. Dev.* **9**, 164-170.

Cattanach, B. M., Burtenshaw, M. D., Rasberry, C. and Evans, E. P. (1993). Large deletions and other gross forms of chromosome imbalance compatible with viability and fertility in the mouse. *Nat. Genet.* **3**, 56-61.

Cattanach, B. M., Peters, J., Ball, S. and Rasberry, C. (2000). Two imprinted gene mutations: three phenotypes. *Hum. Mol. Genet.* **9**, 2263-2273.

Charlier, C., Segers, K., Karim, L., Shay, T., Gyapay, G., Cockett, N. and Georges, M. (2001). The callipyge mutation enhances the expression of coregulated imprinted genes in cis without affecting their imprinting status. *Nat. Genet.* **27**, 367-369.

Constancia, M., Dean, W., Lopes, S., Moore, T., Kelsey, G. and Reik, W. (2000). Deletion of a silencer element in Igf2 results in loss of imprinting independent of H19. *Nat. Genet.* **26**, 203-206.

Cranston, M. J., Spinka, T. L., Elson, D. A. and Bartolomei, M. S. (2001). Elucidation of the minimal sequence required to imprint H19 transgenes. *Genomics* **73**, 98-107.

Croft, J. A., Bridger, J. M., Boyle, S., Perry, P., Teague, P. and Bickmore, W. A. (1999). Differences in the localization and morphology of chromosomes in the human nucleus. *J. Cell Biol.* **145**, 1119-1131.

Cui, H., Niemitz, E. L., Ravenel, J. D., Onyango, P., Brandenburg, S. A., Lobanenkov, V. V. and Feinberg, A. P. (2001). Loss of imprinting of insulin-like growth factor-II in Wilms’ tumor commonly involves altered methylation but not mutations of CTCF or its binding site. *Cancer Res.* **61**, 4947-4950.

Dean, W., Bowden, L., Aitchison, A., Klose, J., Moore, T., Meneses, J. J., Reik, W. and Feil, R. (1998). Altered imprinted gene methylation and expression in completely ES cell- derived mouse fetuses: association with aberrant phenotypes. *Development* **125**, 2273-2282.

DeChiara, T. M., Robertson, E. J. and Efstratiadis, A. (1991). Parental imprinting of the mouse insulin-like growth factor II gene. *Cell* **64**, 849-859.

Eden, S., Constancia, M., Hashimshony, T., Dean, W., Goldstein, B., Johnson, A. C., Keshet, I., Reik, W. and Cedar, H. (2001). An upstream repressor element plays a role in Igf2 imprinting. *EMBO J.* **20**, 3518-3525.

Feil, R., Walter, J., Allen, N. D. and Reik, W. (1994). Developmental control of allelic methylation in the imprinted mouse Igf2 and H19 genes. *Development* **120**, 2933-2943.

Feinberg, A. P. (2000). The two-domain hypothesis in Beckwith-Wiedemann syndrome. *J. Clin. Invest.* **106**, 739-740.

Feinberg, A. P. and Vogelstein, B. (1983). A technique for radiolabeling DNA restriction endonuclease fragments to high specific activity. *Anal. Biochem.* **132**, 6-13.

Ferguson-Smith, A. C., Sasaki, H., Cattanach, B. M. and Surani, M. A. (1993). Parental-origin-specific epigenetic modification of the mouse H19 gene. *Nature* **362**, 751-755.

Ferguson-Smith, A. C. and Surani, M. A. (2001). Imprinting and the epigenetic asymmetry between parental genomes. *Science* **293**, 1086-1089.

Hao, Y., Crenshaw, T., Moulton, T., Newcomb, E. and Tycko, B. (1993). Tumour-suppressor activity of H19 RNA. *Nature* **365**, 764-767.

Hark, A. T., Schoenherr, C. J., Katz, D. J., Ingram, R. S., Levorse, J. M. and Tilghman, S. M. (2000). CTCF mediates methylation-sensitive enhancer-blocking activity at the H19/Igf2 locus. *Nature* **405**, 486-489.

Hill, D. J. (1990). Relative abundance and molecular size of immunoreactive insulin-like growth factors I and II in human fetal tissues. *Early Hum. Dev.* **21**, 49-58.

Hogan, B., Beddington, R., Costantini, F. and Lacy, E. (1994). *Staining for β-galactosidase (*lacZ*) Activity*. New York: CSHL Press.

Holmgren, C., Kanduri, C., Dell, G., Ward, A., Mukhopadhya, R., Kanduri, M., Lobanenkov, V. and Ohlsson, R. (2001). CpG methylation regulates the Igf2/H19 insulator. *Curr. Biol.* **11**, 1128-1130.

Ishihara, K., Hatano, N., Furuumi, H., Kato, R., Iwaki, T., Miura, K., Jinno, Y. and Sasaki, H. (2000). Comparative genomic sequencing identifies novel tissue-specific enhancers and sequence elements for methylation-sensitive factors implicated in Igf2/H19 imprinting. *Genome Res.* **10**, 664-671.

Jones, B. K., Levorse, J. M. and Tilghman, S. M. (1998). Igf2 imprinting does not require its own DNA methylation or H19 RNA. *Genes Dev.* **12**, 2200-2207.

Kaffer, C. R., Srivastava, M., Park, K. Y., Ives, E., Hsieh, S., Batlle, J., Grinberg, A., Huang, S. P. and Pfeifer, K. (2000). A transcriptional insulator at the imprinted H19/Igf2 locus. *Genes Dev.* **14**, 1908-1919.

Kaffer, C. R., Grinberg, A. and Pfeifer, K. (2001). Regulatory mechanisms at the mouse igf2/h19 locus. *Mol. Cell. Biol.* **21**, 8189-8196.

Kanduri, C., Pant, V., Loukinov, D., Pugacheva, E., Qi, C. F., Wolffe, A., Ohlsson, R. and Lobanenkov, V. V. (2000). Functional association of CTCF with the insulator upstream of the H19 gene is parent of origin-specific and methylation-sensitive. *Curr. Biol.* **10**, 853-856.

Kruse, F., Rose, S. D., Swift, G. H., Hammer, R. E. and MacDonald, R. J. (1995). Cooperation between elements of an organ-specific transcriptional enhancer in animals. *Mol. Cell. Biol.* **15**, 4385-4394.

Laird, P. W., Zijderveld, A., Linders, K., Rudnicki, M. A., Jaenisch, R. and Berns, A. (1991). Simplified mammalian DNA isolation procedure. *Nucleic Acids Res.* **19**, 4293.

Leighton, P. A., Saam, J. R., Ingram, R. S., Stewart, C. L. and Tilghman, S. M. (1995a). An enhancer deletion affects both H19 and Igf2 expression. *Genes Dev.* **9**, 2079-2089.

Leighton, P. A., Ingram, R. S., Eggenschwiler, J., Efstratiadis, A. and Tilghman, S. M. (1995b). Disruption of imprinting caused by deletion of the H19 gene region in mice. *Nature* **375**, 34-39.

Li, Y. M., Franklin, G., Cui, H. M., Svensson, K., He, X. B., Adam, G., Ohlsson, R. and Pfeifer, S. (1998). The H19 transcript is associated with polysomes and may regulate IGF2 expression in trans. *J. Biol. Chem.* **273**, 28247-28252.

Maher, E. R. and Reik, W. (2000). Beckwith-Wiedemann syndrome: imprinting in clusters revisited. *J. Clin. Invest.* **105**, 247-252.

Moore, T., Constancia, M., Zubair, M., Bailleul, B., Feil, R., Sasaki, H. and Reik, W. (1997). Multiple imprinted sense and antisense transcripts, differential methylation and tandem repeats in a putative imprinting control region upstream of mouse Igf2. *Proc. Natl. Acad. Sci. USA* **94**, 12509-12514.

Nakagawa, H., Chadwick, R. B., Peltomaki, P., Plass, C., Nakamura, Y. and de La Chapelle, A. (2001). Loss of imprinting of the insulin-like growth factor II gene occurs by biallelic methylation in a core region of H19-associated CTCF-binding sites in colorectal cancer. *Proc. Natl. Acad. Sci. USA* **98**, 591-596.

Paulsen, M., Davies, K. R., Bowden, L. M., Villar, A. J., Franck, O., Fuermann, M., Dean, W. L., Moore, T. F., Rodrigues, N., Davies, K. E. et al. (1998). Syntenic organization of the mouse distal chromosome 7 imprinting cluster and the Beckwith-Wiedemann syndrome region in chromosome 11p15.5. *Hum. Mol. Genet.* **7**, 1149-1159.

Reik, W. and Walter, J. (1998). Imprinting mechanisms in mammals. *Curr. Opin. Genet. Dev.* **8**, 154-164.

Reik, W. and Walter, J. (2001). Genomic imprinting: parental influence on the genome. *Nat. Rev. Genet.* **2**, 21-32.

Szabo, P., Tang, S. H., Rentsendorj, A., Pfeifer, G. P. and Mann, J. R. (2000). Maternal-specific footprints at putative CTCF sites in the H19 imprinting control region give evidence for insulator function. *Curr. Biol.* **10**, 607-610.

Thorvaldsen, J. L., Duran, K. L. and Bartolomei, M. S. (1998). Deletion of the H19 differentially methylated domain results in loss of imprinted expression of H19 and Igf2. *Genes Dev.* **12**, 3693-3702.

Tilghman, S. M. (1999). The sins of the fathers and mothers: genomic imprinting in mammalian development. *Cell* **96**, 185-193.

Tremblay, K. D., Saam, J. R., Ingram, R. S., Tilghman, S. M. and Bartolomei, M. S. (1995). A paternal-specific methylation imprint marks the alleles of the mouse H19 gene. *Nat. Genet.* **9**, 407-413.

Tycko, B. (2000). Epigenetic gene silencing in cancer. *J. Clin. Invest.* **105**, 401-407.